

Thermodynamic curvature of charged black holes with AdS₂ horizons

Aditya Singh¹, Poulami Mukherjee¹ and Chandrasekhar Bhamidipati^{1,2}

¹*School of Basic Sciences, Indian Institute of Technology Bhubaneswar,
Bhubaneswar, Odisha 752050, India*

²*Institute of Physics of the Czech Academy of Sciences and CEICO,
Na Slovance 2, 18221 Prague, Czech Republic*

 (Received 10 August 2023; accepted 17 October 2023; published 13 November 2023)

Sign and magnitude of the thermodynamic curvature provides empirical information about the nature of microstructures of a general thermodynamic system. For charged black holes in anti-de Sitter (AdS), thermodynamic curvature is positive for large charge or chemical potential, and diverges for extremal black holes, indicating strongly repulsive nature. We compute the thermodynamic curvature at low temperatures, for charged black holes with AdS₂ near horizon geometry, and containing a zero temperature horizon radius r_h , in a spacetime which asymptotically approaches AdS_D (for $D > 3$). In the semiclassical analysis at low temperatures, the curvature shows a novel crossover from negative to positive side, indicating the shift from attraction to repulsion dominated regime near $T = 0$, before diverging as $1/(\gamma T)$, where γ is the coefficient of leading low temperature correction to entropy. Accounting for quantum fluctuations, the curvature computed in the canonical ensemble is positive, whereas the one in the grand canonical ensemble, shows a crossover from negative to positive side in the Schwarzsian region. Moreover, the divergence of curvature at $T = 0$ is cured irrespective of the ensemble used, resulting in a universal constant, inversely related to the number of symmetry generators of vacuum AdS₂.

DOI: [10.1103/PhysRevD.108.106011](https://doi.org/10.1103/PhysRevD.108.106011)

I. INTRODUCTION

Thermodynamics of charged black holes in AdS_D spacetimes has been well studied, particularly with the motivation of understanding holographic field theories at finite temperature [1–5]. The presence of an AdS₂ factor in the near horizon geometry which has the form AdS₂ × M_d (where M_d is a compact space with $D = d + 2$) is expected to give universal information about the low energy quantum theories for these black holes. The study of low energy aspects based on the AdS₂ factor has improved our understanding with the advent of Sachdev-Ye-Kitaev models [6–9] and related studies in the low energy limit of string theories [6–41].

A universal property of black holes in AdS_D with charge Q (and also SYK models) is that, there are interesting crossovers at low temperatures, with various thermodynamic quantities receiving nontrivial classical and quantum corrections [42–45]. Energy and charge fluctuations of the low temperature quantum theory lead to a Schwarzsian action [24,42]:

$$I[f, \phi] = -S_0(Q) + \frac{K}{2} \int_0^{1/T} d\tau (\partial_\tau \phi - i(2\pi\mathcal{E}T)\partial_\tau f)^2 - \frac{\gamma}{4\pi^2} \int_0^{1/T} d\tau \{ \tan(\pi T f(\tau)), \tau \}, \quad (1.1)$$

with the following notation for the Schwarzsian

$$\{g(\tau), \tau\} = \frac{g'''}{g'} - \frac{3}{2} \left(\frac{g''}{g'} \right)^2. \quad (1.2)$$

The action is specified in terms of three parameters, namely γ , the compressibility given as

$$K = \left. \frac{dQ}{d\mu} \right|_{T=0}, \quad (1.3)$$

and the electric field at the horizon \mathcal{E} , which can be computed as

$$\frac{dS_0(Q)}{dQ} = 2\pi\mathcal{E}. \quad (1.4)$$

In particular, the dimensionless parameter \mathcal{E} appeared first in the works of Sen [10] while proposing an entropy function for general black holes (see [7,8] for its appearance in complex SYK models). Unlike the zero temperature entropy S_0 and \mathcal{E} , the compressibility K and the coefficient

Published by the American Physical Society under the terms of the Creative Commons Attribution 4.0 International license. Further distribution of this work must maintain attribution to the author(s) and the published article's title, journal citation, and DOI. Funded by SCOAP³.

γ are not universal and depend upon the UV details of the theory. There are further novel modifications of the above model with the inclusion of quantum corrections and also including supersymmetric situations [43–45].

The aim of this paper is to attempt an understanding of the nature of microstructures of such low temperature charged black holes in AdS following recent developments [23,42–46], using the methods of thermodynamic geometry. The main idea of this approach is based on thermodynamic fluctuation theory, which starts from writing the number of microstates of a thermodynamic system as

$$\Omega = e^{\frac{S}{k_B}}, \quad (1.5)$$

where k_B is the Boltzmann constant. One now considers a thermodynamic system I_0 in equilibrium, with a subsystem I in it, in addition to having a couple of independent fluctuating variables, x^i where $i = 1, 2$. The number of microstates in Eq. (1.5) can now be related to the probability $P(x^1, x^2)$ of locating the state of the system somewhere between (x^1, x^2) and $(x^1 + dx^1, x^2 + dx^2)$. According to second law of thermodynamics the pair (x^1, x^2) picks the values that maximize the entropy $S = S_{\max}$. In effect, (x^1, x^2) describe fluctuations around the maximum and the probability around this maximum can be written as [47]:

$$P(x^1, x^2) \propto e^{-\frac{1}{2}\Delta l^2}, \quad (1.6)$$

where the line element which measures thermodynamic distance between two nearby fluctuation states is written as:

$$\Delta l^2 = -\frac{1}{k_B} \frac{\partial^2 S}{\partial x^i \partial x^j} \Delta x^i \Delta x^j. \quad (1.7)$$

The distance is then shorter when the fluctuation between neighboring states is more probable. The thermodynamic curvature R computed from the line element in Eq. (1.7) contains much information, and has been studied for various systems in nature, such as ideal/van der Waals fluids, quantum gases to other Bose/Fermi systems, including the Ising model and black holes [48–64]. The current understanding based on the available empirical data is that repulsive (attractive) interactions of a thermodynamic system turn out to have positive (negative) value of R [47]. R typically diverges at the phase transitions points and has zero crossings at the points where the attractive and repulsive interactions are in balance or in a noninteracting situation.

Thermodynamic geometry of charged black holes in AdS has been well studied in the canonical, grand canonical and also other mixed ensembles in several works (see, e.g., [53,54]). It has also been observed that the curvature R is generally positive for the large black hole branch above a certain critical charge or chemical potential and diverges as

$+1/T$ near $T = 0$, i.e., in the extremal limit. These computations are done for charged black holes in AdS, far away from the horizon. In this work, our motivation is to study the computation of R for charged black holes in AdS, in a certain low temperature regime where the dynamics is governed by corrections to the AdS₂ near horizon geometry. The partition function has been computed recently in both canonical and grand canonical ensembles, carefully taking into account the quantum fluctuations [23,42–46], resolving the mass-gap puzzle [43,44]. As noted above, the thermodynamic variables of black holes in the low temperature limit show certain universal properties, but there are also nonuniversal behaviors, which depend on the how the AdS₂ is embedded in the higher dimensional theory. Here, universality of thermodynamic quantities implies independence of their characteristics on parameters of the geometry far from the AdS₂ near-horizon region. Indeed, the behavior of R in the low temperature limit we find here, is due to the presence of a near horizon AdS₂ geometry, and its nature differs far away from the horizon. More importantly, R diverges on the positive side at $T = 0$, in the semiclassical limit, which is similar to earlier calculations done in the full geometry [53–55]. In addition, the curvature contains a novel crossover from the negative to positive side, which objectively points toward the existence of attractive interactions (bosonic in nature as per our conventions) which develop at low temperatures, i.e., for $T \ll 1/r_h$, before becoming repulsive. Once the quantum corrections to thermodynamic quantities are included, both the curvatures computed in the canonical and grand canonical ensembles and evaluated at $T = 0$, turn out to be equal to a constant. The key take away message is that the quantum corrections to the near horizon nearly AdS₂ geometry cure divergence of the thermodynamic curvature at $T = 0$. This presumably also means that the microstructures are weakly repulsive in nature at $T = 0$, as opposed to the strongly repulsive nature thought of earlier [53–55].

The rest of the paper is as structured as follows. In Sec. II, we set up the notations and collect known details of thermodynamic geometry of charged blackholes in AdS spacetimes. These computations will be for charged black holes in D-dimensions far from the horizon. In particular, we note from Fig. 1, that the thermodynamic curvature is generally positive for large black holes above a certain chemical potential and diverges at $T = 0$. In Sec. III, we perform a computation of the thermodynamic curvature in semiclassical as well as with the inclusion of quantum corrections to thermodynamic quantities. Subsection III A contains the computation of thermodynamic curvature in the semiclassical limit, where the corrections to entropy come from corrections to the AdS₂ geometry [42] and show that there is a novel crossover. The $T = 0$ behavior is unmodified and matches with that seen in Fig. 1. In Sec. III B, we follow [43] and note down the thermodynamic

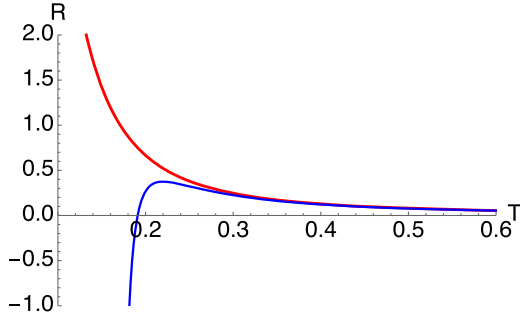


FIG. 1. Thermodynamic curvature of charged black holes in AdS_4 in the (T, μ) plane for $\mu > 1$ (red curve) and $\mu < 1$ (blue curve). The red curve is for $\mu = 1.05$ and the blue curve for $\mu = 0.8$.

quantities in the low temperature limit, where the quantum corrections in both the canonical and grand canonical ensembles can be used to compute the curvature. In the canonical ensemble, the curvature is generally positive, with no crossover and is a positive constant at $T = 0$. In the grand canonical ensemble, the curvature is a positive constant at $T = 0$, but crosses over to the negative side with slight increase of temperature, but still well below $1/r_h$. At $T = 0$, both the curvatures are finite as well as independent of charge, giving a universal constant. We end with remarks in Sec. IV.

II. CHARGED BLACK HOLES IN AdS_d

Let us start with the action of Einstein-Maxwell theory in AdS_{d+2} ($d > 1$) in the presence of a $U(1)$ gauge field with the action [5]:

$$I = \int d^{d+2}x \sqrt{g} \left[-\frac{1}{2\kappa^2} \left(\mathcal{R}_{d+2} + \frac{d(d+1)}{L^2} \right) + F^2 \right], \quad (2.1)$$

where we set $\kappa^2 = 8\pi$ and the gravitational constant $G_N = 1$. \mathcal{R}_{d+2} is the Ricci scalar, with L denoting the

AdS_{d+2} radius. The above theory is known to contain black hole solutions with the metric

$$ds^2 = f(r)d\tau^2 + \frac{dr^2}{f(r)} + r^2 d\Omega_d^2, \quad (2.2)$$

where $d\Omega_d^2$ stands for the metric of the d -dimensional sphere, and

$$f(r) = 1 + \frac{r^2}{L^2} + \frac{q^2}{r^{2d-2}} - \frac{m}{r^{d-1}}. \quad (2.3)$$

As $r \rightarrow \infty$, the metric in Eq. (2.2) goes over to AdS_{d+2} , whereas near the horizon the geometry is $\text{AdS}_2 \times S_d$. The mass is

$$M = \frac{d\omega_d}{16\pi} m = \frac{d\pi^{\frac{d+1}{2}} r^{-d-1} (L^2 r^{2d} + r^{2d+2} + L^2 q^2 r^2)}{8L^2 \Gamma(\frac{d+1}{2})}. \quad (2.4)$$

The grand canonical potential is given as

$$\Omega(T, \mu) = \frac{\omega_d r_0(T, \mu)^{d-1}}{16\pi} \left(1 - \frac{r_0(T, \mu)^2}{L^2} \right) - \frac{\omega_d (d-1) \mu^2 r_0(T, \mu)^{d-1}}{2d}. \quad (2.5)$$

from which the entropy and charge can be obtained to be

$$S(T, \mu) = \frac{\pi^{\frac{d+1}{2}} r_0^d}{2\Gamma(\frac{d+1}{2})}, \quad (2.6)$$

$$Q(T, \mu) = \frac{\sqrt{(d-1)d}\omega_d}{4\sqrt{2\pi}} q = \frac{(d-1)\pi^{\frac{d-1}{2}} \mu r_0^{d-1}}{2\Gamma(\frac{d+1}{2})}, \quad (2.7)$$

where $\omega_d = \frac{2\pi^{\frac{d+1}{2}}}{\Gamma(\frac{d+1}{2})}$. Focussing on the large black hole branch, the specific heat can be written as,

$$C_\mu = \frac{d^2 \pi^{\frac{d+3}{2}} L^2 T \left(\frac{\sqrt{dL^2(d^3(2\mu^2-1) - 2d^2\mu^2 + d(-2\mu^2 + 4\pi^2 L^2 T^2 + 1) + 2\mu^2) + 2\pi d L^2 T}}{d(d+1)} \right)^d}{\Gamma(\frac{d+1}{2}) \sqrt{dL^2(d^3(2\mu^2-1) - 2d^2\mu^2 + d(-2\mu^2 + 4\pi^2 L^2 T^2 + 1) + 2\mu^2)}}, \quad (2.8)$$

Black holes in the fixed potential ensemble are known to show distinct behavior for $\mu < 1$ and $\mu > 1$ [5] and our interest is in the later regime where extremal limit can be taken. Using the grand potential, a thermodynamic line element can be constructed as [47,53,54,64],

$$\Delta l^2 = -\frac{1}{T} \frac{\partial^2 \Omega(T, \mu)}{\partial x^i \partial x^j} \Delta x^i \Delta x^j, \quad (2.9)$$

where the fluctuation coordinates x^i are chosen as (T, μ) . The above line element is conformally related to the one in Eq. (1.7). The curvature following from it can be computed straightforwardly, though the resulting expression is quite long to express here. We instead show the result in Fig. 1, which matches with the earlier computations [53,54].

The low temperature behavior for $\mu > 1$ is given below which will be useful later:

$$R = \frac{3\sqrt{3}(2\mu^2 - 1)}{4\pi^2(\mu^2 - 1)^{3/2}L^3T} - \frac{3(6\mu^2 - 1)}{4(\pi(\mu^2 - 1)^2L^2)} + \frac{(4\sqrt{3}\mu^2 + \sqrt{3})T}{2(\mu^2 - 1)^{5/2}L} + O(T^2). \quad (2.10)$$

We note that R is positive and diverges as $T \rightarrow 0$, indicating strongly repulsive type interactions of microstructures.

III. LOW TEMPERATURE NEARLY AdS₂

Various thermodynamic quantities of the extremal black hole can be extracted as below. At sufficiently low temperatures, nonconstant modes on S_d are not excited and certain universal features can be obtained. In the fixed potential case, the expressions in the previous section were for general values of T and μ and in this section, following [42], the low temperature expressions (at fixed $\mu = \mu_0$) can be obtained by writing r_0 as

$$r_0 = r_h(\mu_0) + \frac{2\pi L^2}{d+1}T + O(T^2) \quad (3.1)$$

where

$$r_h \equiv L \left[\frac{(d-1)(\mu_0^2 8\pi(d-1) - d)}{d(d+1)} \right]^{1/2}, \quad (3.2)$$

is the zero temperature horizon radius and $\mu_0 = \mu|_{T=0}$. The expansion in Eq. (3.2), allows writing extremal value of entropy as

$$S_0 = \frac{2\pi\omega_d}{8\pi} r_h^d, \quad (3.3)$$

where ω_d is the area of d -dimensional unit sphere. Note that the entropy S_0 is given terms of the area of the horizon in the d -dimensional geometry. Compressibility can be written as

$$K = \frac{(d-1)\omega_d r_h^{d-3} [d(d+1)r_h^2 + (d-1)^2L^2]}{(d+1)}. \quad (3.4)$$

Extremal value of charge can be expressed in terms of μ_0 as

$$Q = \frac{(d^2 - 1)\pi^{\frac{d+1}{2}}\mu_0 \left(\frac{L\sqrt{d(d^2-1)(d(2\mu_0^2-1)-2\mu_0^2)}}{d(d+1)} \right)^{d-1}}{2(d+1)\Gamma(\frac{d+1}{2})}. \quad (3.5)$$

The low temperature analysis can also be done in the canonical ensemble at constant Q . Note that in the extremal limit, the function $f(r)$ in Eq. (2.3) has a double zero at r_h .

The key idea in studying the near-extremal black holes is to divide their geometry into a near horizon and a far away region, such that both the regions overlap in the bulk [26,43]. For the near horizon region at fixed temperature

and charge situation, one can expand the radius (in four dimensions) as [42,43]

$$r = r_h + \delta r_h, \quad \delta r_h = 2\pi T r_2^2 + \dots, \quad (3.6)$$

where $r_2 \equiv \frac{Lr_h}{\sqrt{L^2+6r_h^2}}$ is the radius of AdS₂. The near horizon region is at a distance $r - r_h \ll r_h$, and is nearly AdS₂ \times S². Considering the metric in Eq. (2.3) one can define $\rho = r - r_h$ and obtain the near-horizon region metric to be

$$ds^2 = \frac{(\rho^2 - 4\pi^2 T^2 r_2^4)}{r_2^2} d\tau^2 + \frac{r_2^2}{(\rho^2 - 4\pi^2 T^2 r_2^4)} d\rho^2 + (r_h + \rho)^2 d\Omega_2 \quad (3.7)$$

where the first two terms stand for the finite temperature AdS₂, and the last term corresponds to the metric of a sphere with an almost constant radius r_h . The additional slowly varying term is the size of the sphere, which breaks the symmetries of AdS₂, dominating the dynamics at low-temperatures [16,19]. As discussed in [42,43], for $2\pi T r_2^2 < \rho \ll r_h$, the geometry approaches vacuum AdS₂, whereas the region $T r_h^2 < \rho \ll r_h$ is the Schwarzsian regime.

A. Semiclassical analysis

In the nearly AdS₂ spacetime the thermodynamic quantities receive corrections. The free energy in the fixed charge ensemble $F = \Omega + \mu Q$ gets corrected to order T^2 as [42,65]:

$$F = \frac{\pi^{\frac{d-1}{2}} r_h^d \left(\frac{d^2 r_h}{(d-1)L^2} + d \left(\frac{1}{r_h} - \frac{2\pi^2 L^2 r_h T^2}{(d-1)^2 L^2 + d(d+1)r_h^2} \right) - 2\pi T \right)}{4\Gamma(\frac{d+1}{2})}. \quad (3.8)$$

The entropy in this limit acquires corrections at low temperature as

$$S(Q, T \rightarrow 0) = S_0(Q) + \gamma T + \dots, \quad (3.9)$$

where $\gamma = M_{SL(2)}^{-1}$ is the conformal symmetry breaking scale. $S_0(Q)$ is the zero temperature entropy and is nonzero, as given in Eq. (3.3). The coefficient can be deduced from the corrections to the near horizon AdS₂ geometry [9,16,17,19] as

$$\gamma = \frac{d\pi^{\frac{d+3}{2}} L^2 r_h^{d+1}}{\Gamma(\frac{d+1}{2})((d-1)^2 L^2 + d(d+1)r_h^2)}. \quad (3.10)$$

Due to the above scaling of entropy with temperature as in Eq. (3.9), it was believed that the statistical description breaks down at temperatures lower than $1/\gamma$. The scale $M_{SL(2)}$ is now understood as the energy at which the

(approximate) near horizon conformal symmetry of AdS_2 is broken. This becomes evident once the quantum corrections are taken into account [43]. For now, we continue with the semiclassical analysis and return to consider the quantum corrected thermodynamic quantities in the next subsection. The low temperature behavior of the chemical potential μ at leading order can be written as [42]

$$\mu(T) = \mu_0 - 2\pi\mathcal{E}T + \dots, \quad (3.11)$$

where

$$2\pi\mathcal{E} = \frac{\sqrt{2\pi L r_h} \sqrt{d((d-1)L^2 + (d+1)r_h^2)}}{(d-1)^2 L^2 + d(d+1)r_h^2}. \quad (3.12)$$

The second term in Eq. (3.11) is purely the contribution at the boundary of AdS_2 and its contribution at the AdS_{d+2} boundary can be computed in the presence of time diffeomorphisms and gives the second term in Eq. (1.1). We will see in the following section that Eq. (3.11) gets corrected further due to quantum fluctuations and we will use the temperature dependent terms there to compute the curvature.

We can compute the thermodynamic curvature straightforwardly in both the canonical and grand canonical ensembles, but we prefer the later here, for comparison with the results in the previous section. While using zero temperature relations, we will continue to express the thermodynamic relations in terms of either r_h , Q or μ_0 as per convenience as all these are constants, related to each other. The particular length ratio L/r_h is kept fixed as the temperature is lowered in the limit $T \rightarrow 0$. We will set $L = 1$ in the plots. Evaluating the curvature following from the metric in Eq. (2.9), the expression for the four dimensional case is

$$R = \frac{\sqrt{3}(3(1-2\mu_0^2)^4 - 4\pi^2(4\mu_0^6 + 8\mu_0^4 - 11\mu_0^2 - 1)L^2T^2)}{4\pi^2(\mu_0^2 - 1)^{3/2}(2\mu_0^2 - 1)^3L^3T}. \quad (3.13)$$

The above expression has been written in terms of μ_0 for convenience, and can be converted to the fluctuating variable Q using Eq. (3.5). The first few terms of Eq. (3.13) close to $T = 0$ are

$$R = \frac{3\sqrt{3}(2\mu_0^2 - 1)}{4\pi^2(\mu_0^2 - 1)^{3/2}L^3T} - \frac{\sqrt{3}(4\mu_0^6 + 8\mu_0^4 - 11\mu_0^2 - 1)T}{(\mu_0^2 - 1)^{3/2}(2\mu_0^2 - 1)^3L} + O(T^2) \quad (3.14)$$

The general result for curvature in Fig. 1 is positive all along and approaches zero at high temperatures. However, the low temperature curvature in Eq. (3.13) behaves slightly differently, as seen in Fig. 2. As the temperature is lowered (and still much below the energy scale $1/r_h$), the curvature

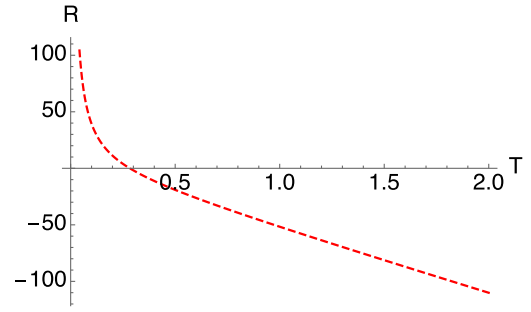


FIG. 2. Thermodynamic curvature for charged black holes with near horizon AdS_2 geometry at low temperature. The curvature crosses over from negative to positive side at $T = 0.282$ for $Q = 0.2$ (or equivalently $\mu_0 = 1.052$).

can be negative, before resuming the positive behavior and subsequent divergence as $T \rightarrow 0$. The $T = 0$ behavior is universal in this limit. That is, the first term of thermodynamic curvature in the general expression in Eq. (2.10) and the low temperature computation in Eq. (3.14) agree exactly, showing the typical $1/T$ divergence in the extremal limit. In fact, we note that the coefficient of leading $1/T$ term in either of these low temperature series for curvature is exactly $1/\gamma$.

Based on the empirical understanding of thermodynamic curvature, the points of crossover of R indicate shift of the nature of collective interactions of microstructures from attraction dominated (negative R) to repulsion dominated (positive R) at a temperature, which is in the physical region of interest. That is, the shaded region in Fig. 3 where the black hole also shows a crossover and the description in terms of an effective action governed by the Schwarzian starts becoming feasible (see Fig. 2 in [42]). The zero crossing of the thermodynamic curvature in Eq. (3.13) occurs at

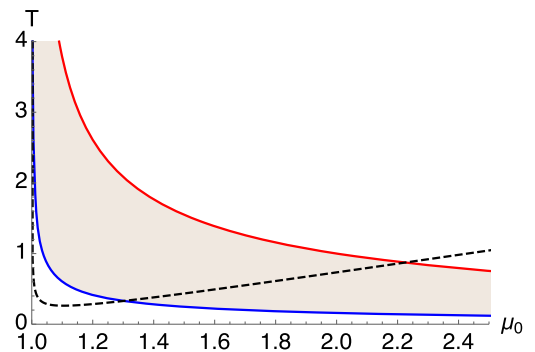


FIG. 3. The red and blue curves represent $1/r_h$ and $1/(2\pi r_h)$ respectively, with the shaded region in between them marking the Schwarzian regime. The dashed curve represents the temperature at which the curvature [Eq. (3.15)] has zeroes as a function of μ_0 . $d = 2$ for all the cases.

$$T_{R=0} = \frac{\sqrt{3}(1 - 2\mu_0^2)^2}{2\pi\sqrt{4\mu_0^6 + 8\mu_0^4 - 11\mu_0^2 - 1L}} \quad (3.15)$$

as also seen in Fig. 3, happening at temperatures much lower than $1/r_h$, and for some range of charges, even happening below $1/(2\pi r_h)$, which is the nearly AdS₂ region. Of course, the crossing of R shown in Fig. 3 cannot be trusted at temperature comparable to $1/r_h$.

We should probably also mention that our computations in this paper are limited to the situation corresponding to a large chemical potential, as in [42], such that the horizon radius in Eq. (3.2) exists. Hence, the thermodynamic curvature does not capture phase transitions or critical points.

B. Quantum corrections

In this subsection, we follow the analysis in [43], where the corrections to thermodynamic quantities coming from quantum fluctuations were computed for Reissner-Nordström near-extremal black holes at low temperatures. One of the key findings of [43] is that in the fixed charge sector, the density of states of the system does not show a gap, but rather a continuum of states, for the case of nonsupersymmetric black holes. The computed partition function in the canonical and grand canonical ensembles shows that the low energy limit is well captured by two dimensional Jackiw-Teitelboim (JT) gravity, which is coupled to a $U(1)$ gauge field and other gauge fields coming from dimensional reduction. We first compute the thermodynamic curvature in the canonical ensemble and then in the grand canonical ensemble.

The partition function in the fixed charge ensemble was shown in [43] to be

$$Z_{\text{RN}}[T, Q] = (\gamma T)^{3/2} e^{\pi r_h^2 - M_0(Q)/T + 2\pi^2 \gamma T}. \quad (3.16)$$

Here, the terms in the exponential correspond respectively to the extremal entropy, extremal mass and the semi-classical corrections near extremality. We should mention that γ in the above expression is same as the one appearing in Eq. (3.10), but its origin is tied to the value of the dilation evaluated from the boundary terms originating in the overlap region of near and far regimes of the near extremal black [43]. The important piece for the current analysis of course is the prefactor in Eq. (3.16), which follows from the gravitational one-loop contribution of the JT mode, and also dominates the low temperature behavior of thermodynamic quantities to follow. For our purposes, the entropy computed from the corrected free energy following from Eq. (3.16) is

$$S(Q, T) = S_0(Q) + \gamma T + \frac{k}{2} \log(\gamma T). \quad (3.17)$$

The leading two terms are same as the ones noted in Eq. (3.9), where $k = 3$ for the general case considered in [43], but we leave it arbitrary for reasons to be clear below. The specific heat following from Eq. (3.17) is

$$C = \frac{1}{18} T \left(\frac{9k}{T} + \frac{2\sqrt{6}\pi^{7/4} L^{5/2} (\sqrt{\pi L^2 + 3Q^2} - \sqrt{\pi} L)^{3/2}}{\sqrt{\pi L^2 + 3Q^2}} \right), \quad (3.18)$$

where one notices that the quantum corrections regulate the expression in the $T = 0$ limit giving a constant $k/2$. The chemical potential is found to be

$$\begin{aligned} \mu = & -\frac{\sqrt{L^2 + 3r_h^2}}{8\sqrt{\pi} L r_h (L^2 + 6r_h^2)^3} \\ & \times (24\pi^2 L^4 r_h^3 T^2 (L^2 + 2r_h^2) + L^2 T (L^2 + 6r_h^2) \\ & \times (L^2 (8\pi r_h^2 + 27) + 6r_h^2 (8\pi r_h^2 + 9)) - 4r_h (L^2 + 6r_h^2)^3). \end{aligned} \quad (3.19)$$

The partition function in the fixed potential ensemble reads [43]

$$Z_{\text{RN}}[T, \mu] = e^{\mu \frac{Q_0}{T} + S_0(Q_0) - M_0(Q_0)/T} (\gamma T)^{k/2} e^{2\pi^2 \gamma T} Z_{U(1)}, \quad (3.20)$$

where $Z_{U(1)}$ is the contribution of the $U(1)$ mode, which can change the power k depending on the regime of temperature being studied. Here, one remembers that in the grand canonical ensemble, μ_0 is taken to be function of only Q , which is the zero temperature contribution from Eq. (3.19) and can also be obtained by inverting Eq. (3.5). We ignore it for now, as does not induce any change to the qualitative behavior of the curvature to be discussed below. With the above partition functions in both ensembles, one can now do the computation of thermodynamic curvatures in both the canonical and the grand canonical ensembles. For the canonical ensemble, one can write a metric as [47,53,54,64],

$$dl^2 = -\frac{1}{T} \frac{\partial^2 F}{\partial T^2} (dT)^2 + \frac{1}{T} \frac{\partial^2 F}{\partial Q^2} (dQ)^2, \quad (3.21)$$

whereas for the grand canonical, one can use the same metric noted earlier in Eq. (2.9). The thermodynamic curvature can be computed analytically as such in both the ensembles, though the expressions are quite involved and are given in the Appendix. Here, the expression for curvature can be expressed in terms of Q as well. The behavior of curvatures in both the ensembles is summarized in Fig. 4, which shows major changes due to quantum corrections coming from the JT mode. First, the thermodynamic curvature at $T = 0$ does not diverge anymore, irrespective of the ensemble used, and actually gives $R_{T=0} = 1/k$, which is a universal constant independent

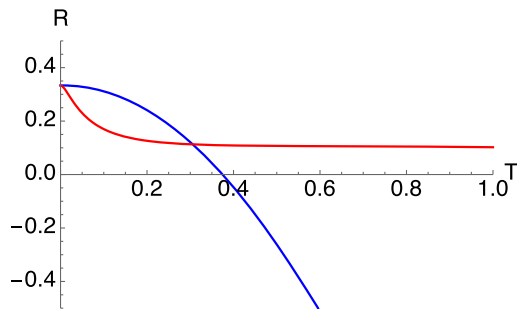


FIG. 4. Red and blue curves represent respectively, the thermodynamic curvatures in canonical and grand canonical ensembles in four dimensions for $Q = 2$, $L = 1$. The value at $T = 0$ is $R = 1/k$ where we took $k = 3$ here.

of charge. This is in stark contrast to the divergence seen in the thermodynamic curvature in earlier studies for full AdS_D background [51,53–55], and also the semiclassical analysis in the nearly AdS_2 near horizon geometry in the last subsection. Thus, the quantum corrections following from the JT mode regularise the divergence of thermodynamic curvature in the low temperature limit. From the existing results on Ruppeiner geometry, one concludes that a small positive constant value of thermodynamic curvature at $T = 0$ might presumably mean the presence of weakly interacting repulsive nature of the system. In the grand canonical ensemble, the thermodynamic curvature starts out as highly negative indicating the possibility of strongly interacting microstructure behavior akin to a bosonic system. This is followed by a point where there is a crossover from negative to positive side at a temperature between $1/(2\pi r_h)$ and $1/r_h$ (shaded region in Fig. 5). This crossing was already seen in the semiclassical analysis in Fig. 3, but there it started showing up from much lower temperatures in the AdS_2 regime. Here, with quantum corrections, the zero crossings of curvature occur precisely within the shaded region, i.e., where the Schwarzian

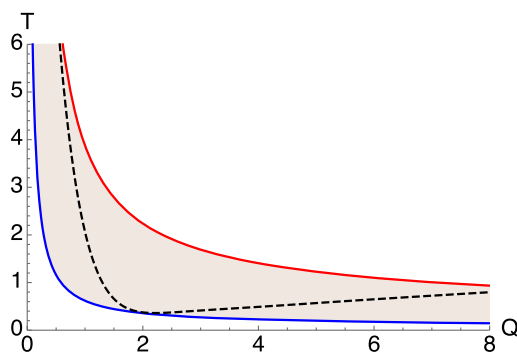


FIG. 5. The red and blue curves represent $1/r_h$ and $1/(2\pi r_h)$ respectively, with the shaded region in between them marking the Schwarzian regime. The dashed curve represents the temperature at which the curvature in the grand canonical ensemble has zeroes as a function of charge Q (or equivalently the chemical potential μ_0).

description starts becoming relevant, and the black hole is expected to have a crossover [42]. One hopes the quantum corrected temperature of crossover found here is more reliable. Also, the quantum corrected behavior of thermodynamic curvature cannot be obtained directly by taking a naive $T = 0$ limit of the results in the full AdS_D geometry [47,53,54,64].

We should mention that the curvature in the canonical ensemble also has a crossover for some range of charges, but it happens at temperatures well above $1/r_h$, where the analysis is not reliable, and hence are not included in the plots. All these features are also happen below the conformal symmetry breaking scale $M_{SL(2)}$, which is not a problem here as there is no mass gap. Due to the arguments in [43] for nonsupersymmetric black holes, the thermodynamic analysis in this limit is justified.

IV. CONCLUSIONS

Charged black holes in AdS have long been used as holographic models for strongly interacting quantum systems at finite density [39]. Close to the boundary, the geometry asymptotes to AdS_D , where the usual AdS/CFT relations hold, giving an understanding of bulk properties in terms of field theory in $D - 1$ spacetime dimensions. The low temperature correlations (for $D > 3$) however were linked to the presence of the near horizon AdS_2 geometry alone [29]. More recently, following examples of the SYK model, interesting one dimensional Schwarzian action has been studied [16,17,19,23,24,35,36], which has allowed novel computation of quantum properties, in comparison to the AdS_D approach. The effective one dimensional action has also been obtained from the low energy limit of the Einstein-Maxwell theory which contains the charged black holes in asymptotically AdS_D spacetime [42–45]. In particular, at low temperatures, the black holes exhibit interesting crossovers to the Schwarzian regime. The semiclassical analysis is now supplemented by the quantum corrections, which play a crucial role in resolving the mass gap puzzle in the non-supersymmetry near extremal black holes [43].

Purely from thermodynamics point of view, Ruppeiner geometry is known to give reliable results on the nature of microscopic interactions of degrees of freedom, for a wide range of systems, starting from black holes to quantum gases. For the case of charged black holes in full AdS_D geometry, the key features of thermodynamic curvature are as follows. The curvature shows one negative divergence at the critical point of phase transition and a positive divergence at $T = 0$ [53–55]. The negative to positive crossing of the curvature happens exactly at the point where the Gibbs free energy also changes sign and this corresponds to Hawking-Page transition. Except for the behavior of curvature at $T = 0$, all the other features can be understood independently either from the free energy or the behavior of other thermodynamic quantities. Following recent developments in [42–45] which showed that the thermodynamic quantities of charged black

holes at low temperatures undergo nontrivial changes at the semiclassical and also due to quantum fluctuations, it is imperative to revisit the computation of thermodynamic geometry in these regimes. In this paper, we performed a computation of the curvature R in the low temperature regime, both in the semiclassical limit as well as after including quantum corrections, in the nearly AdS_2 space-time. It is then useful to compare the behavior of thermodynamic curvature of charged black holes in the full AdS_D geometry [53–55] with the computation done here in the low temperature regime.

First, in the semiclassical limit, as the temperature is lowered, keeping the charge fixed (and sufficiently large), R shows an additional new crossover from negative to positive side (before diverging as $\frac{1}{r_h}$), in the region where the temperature is much less than $1/r_h$ [and also possibly below $1/(2\pi r_h)$]. This is also the region where the black hole undergoes interesting crossovers [42]. Let us note that the above crossovers are particularly low energy phenomena, where the black holes in AdS_D geometry are better approximated as $\text{AdS}_2 \times M_d$ (where M_d is a compact space with $D = d + 2$). The Einstein-Maxwell action in the former geometry can be rewritten in the later background, to obtain an effective dilaton gravity theory in two dimensions, as described in [16,17,19,23,24,35,36]. As one moves away from the AdS_2 throat region, this two dimensional theory exhibits novel conformal symmetry breaking behavior and becomes dynamical, which might be understood in terms of holographic renormalization group flow. Such studies are expected to throw more light on the connection between the behavior of thermodynamic curvature in the full AdS_D geometry and its low energy behavior presented here. This should be pursued in the future.

Actually, for the charged black holes in AdS, if we take the temperature to be extremely low, the theory is essentially topological [16,17,19,23,24,35,36]. The nearly AdS_2 gravity with a finite temperature can be understood in terms of JT gravity with a boundary Schwarzian action, resulting in the $-\frac{k}{2}T \log T$ term in the free energy. This term resulting from quantum corrections, dominates the low temperature behavior and in our case renders the thermodynamic curvatures finite. In fact, with quantum corrections, the curvature is regular with no divergence at any low temperature. In the grand canonical ensemble, the thermodynamic curvature continues to show a smooth crossover for a wide range of charges, for temperatures which precisely lie between $1/(2\pi r_h)$ and $1/r_h$. The crossover presumably corresponds to a shift in the nature of dominant interactions of microstructures from bosonic (negative R) to fermionic (positive R) type, which should be understood better. Furthermore, the value of the curvature at $T = 0$ is a universal constant, inversely related to the number of $SL(2)$ generators. For the present case, it is tempting to speculate that the interactions of microstructures are weakly repulsive as the temperature nears zero, as opposed to the strongly

repulsive nature anticipated earlier from the analysis of thermodynamic curvature in the full AdS_D geometry [53–55]. In the supersymmetric case, this number should equal the number of generators of the full supergroup. There are other instances where such universal constants have appeared in special limits of thermodynamic curvature with interesting physical interpretations [63,66,67], but were all at finite temperature.

Another related remark concerns the applicability of thermodynamic geometry to low temperature situations. Thermodynamic curvature has thus far been studied with particular emphasis on the phase transitions and critical phenomena, which are all phenomena at finite temperature. It is then interesting that the value of thermodynamic curvature at $T = 0$ found here, is inversely related to the power k of temperature in the partition function in Eq. (3.16), which for the present case is known to be $k = 3$. This is also the number of symmetry generators of the $SL(2)$ group which is preserved by the pure AdS_2 geometry.¹ It points to a deeper connection of thermodynamic curvature to the symmetry generators and should be explored further by examining similar issues for supersymmetric black holes. Given that near extremal black holes in both supersymmetric (where additional BPS conditions are possible) and nonsupersymmetric theories have a ground state degeneracy with nonzero entropy, it may be possible to set up thermodynamic geometry for quantum systems at zero temperature.

Some further avenues which can be explored are as follows. Black holes in higher derivative gravity are known to give nontrivial corrections to the entropy of black holes, both in supersymmetric and nonsupersymmetric situations. It is important to study their thermodynamic geometry in the near horizon limit, with corrections to AdS_2 geometry as done here. Second, it has been suggested that the mass gap does exist for BPS black holes in supersymmetric theories [44,45], it is then interesting to check whether the thermodynamic curvature in either of the ensembles studied here, has any new behavior.

ACKNOWLEDGMENTS

We thank Matthew Heydeman, Hao Geng and Sudipta Mukherji for helpful correspondence and comments on the draft. A. S. wishes to thank the Council of Scientific and Industrial Research (CSIR), Government of India, for financial support. P.M. thanks IIT Bhubaneswar for Institute fellowship. C.B. thanks the DST (SERB), Government of India, for financial support through the Mathematical Research Impact Centric Support (MATRICS) Grant No. MTR/2020/000135 and the Institute of Physics of the Czech Academy of Sciences and CEICO, Prague, for warm hospitality.

¹We thank Matthew Heydeman for pointing out the connection of k to the symmetry generators.

APPENDIX: EXPRESSIONS FOR THERMODYNAMIC CURVATURES

Here, we note down the thermodynamic curvatures found in Sec. III for case of low temperature nearly AdS₂. Curvature in the canonical ensemble is computed using the line element in Eq. (3.21), in terms of the fluctuation variables (T, Q) , but expressed below in terms of (T, r_h) for clarity. r_h can be converted in terms of charge Q , using Eq. (3.2). The expression is,

$$R = A/B,$$

$$\begin{aligned}
A = & 36r_h^3(6r_h^2 + 1)^2(248832\pi^2 r_h^{18} T(\pi^2 T^2 + 21) + 2239488r_h^{17}(2\pi^2 T^2 + 3) \\
& + 20736r_h^{16} T(14\pi^4 T^2 + 126\pi^2 + 243) + 15552r_h^{15}(15\pi^4 T^4 - 8\pi^3 T^2 + 552\pi^2 T^2 + 252) \\
& + 3456r_h^{14} T(4\pi^4 T^2 + 3\pi^2(81T^2 + 70) - 54\pi + 3159) - 2304r_h^{13}(7\pi^5 T^4 - 270\pi^4 T^4 + 45\pi^3 T^2 \\
& - 2565\pi^2 T^2 - 567) - 192r_h^{12} T(112\pi^6 T^4 + 372\pi^4 T^2 + 270\pi^3 T^2 - 9\pi^2(1377T^2 + 70) + 972\pi - 46656) \\
& - 864r_h^{11}(12\pi^5 T^4 - 529\pi^4 T^4 + 40\pi^3 T^2 - 2280\pi^2 T^2 - 315) - 32r_h^{10} T(472\pi^6 T^4 + 858\pi^4 T^2 \\
& + 1728\pi^3 T^2 - 27\pi^2(2727T^2 + 14) + 2430\pi - 118827) - 64r_h^9(29\pi^5 T^4 - 2070\pi^4 T^4 + 90\pi^3 T^2 \\
& - 5400\pi^2 T^2 - 567) - 32r_h^8 T(84\pi^6 T^4 + 121\pi^4 T^2 + 702\pi^3 T^2 - 3\pi^2(11745T^2 + 7) + 540\pi - 29160) \\
& - 12r_h^7(8\pi^5 T^4 - 1119\pi^4 T^4 + 40\pi^3 T^2 - 2568\pi^2 T^2 - 252) - 8r_h^6 T(24\pi^4 T^2 + 552\pi^3 T^2 \\
& - \pi^2(35667T^2 + 2) + 270\pi - 17091) - 16r_h^5(\pi^3 T^2 - 69\pi^2 T^2 - 9) - 4r_h^4 T(106\pi^3 T^2 \\
& - 9567\pi^2 T^2 + 36\pi - 2916) + 2r_h^2 T(-8\pi^3 T^2 + 1287\pi^2 T^2 - 2\pi + 261) + 4478976\pi^2 r_h^{20} T \\
& + 5038848r_h^{19} + 3r_h^3 + 9(8\pi^2 T^3 + T)) \\
B = & (8\pi^2 r_h^3 T + 18r_h^2 + 3)^2(432r_h^9(\pi^2 T^2 + 12) + 144r_h^7(4\pi^2 T^2 + 9) + 12r_h^5(7\pi^2 T^2 + 12) \\
& + r_h^3(6 - 24\pi^2 T^2) + 3888r_h^8 T - 72(2\pi - 81)r_h^6 T - 24(2\pi - 99)r_h^4 T + (306 - 4\pi)r_h^2 T \\
& + 7776r_h^{11} + 9T)^2.
\end{aligned} \tag{A1}$$

Similarly, the thermodynamic curvature in the grand canonical ensemble is computed in terms of the fluctuation variables (μ_0, T) using the line element in Eq. (2.9), but can also be converted in terms of the extremal charge Q using Eq. (3.5). The expression is,

$$R = A/B,$$

$$\begin{aligned}
A = & -27k(8\pi\mu_0^2 - 1)(8\pi^2(128\pi^3\mu_0^6 + 96\pi^2\mu_0^4 - 46\pi\mu_0^2 - 1)L^2 T^2 - 3(1 - 8\pi\mu_0^2)^4) - 48\sqrt{3}\pi^2 \\
& \times (4\pi\mu_0^2 - 1)^{3/2} L^3 T(4\pi^2(256\pi^3\mu_0^6 + 128\pi^2\mu_0^4 - 44\pi\mu_0^2 - 1)L^2 T^2 - 3(1 - 8\pi\mu_0^2)^4), \\
B = & (8\pi\mu_0^2 - 1)^3(9k(8\pi\mu_0^2 - 1) + 8\sqrt{3}\pi^2(4\pi\mu_0^2 - 1)^{3/2} L^3 T)^2.
\end{aligned} \tag{A2}$$

-
- [1] J. M. Maldacena, The large N limit of superconformal field theories and supergravity, *Adv. Theor. Math. Phys.* **2**, 231 (1998).
- [2] S. S. Gubser, I. R. Klebanov, and A. M. Polyakov, Gauge theory correlators from non-critical string theory, *Phys. Lett. B* **428**, 105 (1998).
- [3] E. Witten, Anti-de sitter space and holography, *Adv. Theor. Math. Phys.* **2**, 253 (1998).
- [4] E. Witten, Anti-de sitter space, thermal phase transition, and confinement in gauge theories, *Adv. Theor. Math. Phys.* **2**, 505 (1998).
- [5] A. Chamblin, R. Emparan, C. V. Johnson, and R. C. Myers, Charged AdS black holes and catastrophic holography, *Phys. Rev. D* **60**, 064018 (1999).
- [6] S. Sachdev and J. Ye, Gapless spin-fluid ground state in a random quantum Heisenberg magnet, *Phys. Rev. Lett.* **70**, 3339 (1993).
- [7] A. Georges, O. Parcollet, and S. Sachdev, Quantum fluctuations of a nearly critical Heisenberg spin glass, *Phys. Rev. B* **63**, 134406 (2001).
- [8] S. Sachdev, Bekenstein-Hawking entropy and strange metals, *Phys. Rev. X* **5**, 041025 (2015).

- [9] A. Y. Kitaev, Entanglement in strongly-correlated quantum matter, *Talks at KITP* (University of California, Santa Barbara, 2015).
- [10] A. Sen, Black hole entropy function and the attractor mechanism in higher derivative gravity, *J. High Energy Phys.* **09** (2005) 038.
- [11] A. Dabholkar, Exact counting of black hole microstates, *Phys. Rev. Lett.* **94**, 241301 (2005).
- [12] A. Dabholkar, A. Sen, and S. P. Trivedi, Black hole microstates and attractor without supersymmetry, *J. High Energy Phys.* **01** (2007) 096.
- [13] A. Sen, Entropy function and $\text{AdS}_2/\text{CFT}_1$ correspondence, *J. High Energy Phys.* **11** (2008) 075.
- [14] S. Sachdev, Holographic metals and the fractionalized Fermi liquid, *Phys. Rev. Lett.* **105**, 151602 (2010).
- [15] A. Dabholkar, J. Gomes, and S. Murthy, Nonperturbative black hole entropy and Kloosterman sums, *J. High Energy Phys.* **03** (2015) 074.
- [16] A. Almheiri and J. Polchinski, Models of AdS_2 backreaction and holography, *J. High Energy Phys.* **11** (2015) 014.
- [17] A. Almheiri and B. Kang, Conformal symmetry breaking and thermodynamics of near-extremal black holes, *J. High Energy Phys.* **10** (2016) 052.
- [18] J. Maldacena and D. Stanford, Remarks on the Sachdev-Ye-Kitaev model, *Phys. Rev. D* **94**, 106002 (2016).
- [19] J. Maldacena, D. Stanford, and Z. Yang, Conformal symmetry and its breaking in two dimensional nearly anti-de-Sitter space, *Prog. Theor. Exp. Phys.* **2016**, 12C104 (2016).
- [20] J. Engelsöy, T. G. Mertens, and H. Verlinde, An investigation of AdS_2 backreaction and holography, *J. High Energy Phys.* **07** (2016) 139.
- [21] K. Jensen, Chaos and hydrodynamics near AdS_2 , *Phys. Rev. Lett.* **117**, 111601 (2016).
- [22] W. Fu, D. Gaiotto, J. Maldacena, and S. Sachdev, Supersymmetric Sachdev-Ye-Kitaev models, *Phys. Rev. D* **95**, 026009 (2017).
- [23] D. Stanford and E. Witten, Fermionic localization of the Schwarzian theory, *J. High Energy Phys.* **10** (2017) 008.
- [24] R. A. Davison, W. Fu, A. Georges, Y. Gu, K. Jensen, and S. Sachdev, Thermoelectric transport in disordered metals without quasiparticles: The Sachdev-Ye-Kitaev models and holography, *Phys. Rev. B* **95**, 155131 (2017).
- [25] A. Gaikwad, L. K. Joshi, G. Mandal, and S. R. Wadia, Holographic dual to charged SYK from 3D gravity and Chern-Simons, *J. High Energy Phys.* **02** (2020) 033.
- [26] P. Nayak, A. Shukla, R. M. Soni, S. P. Trivedi, and V. Vishal, On the dynamics of near-extremal black holes, *J. High Energy Phys.* **09** (2018) 048.
- [27] U. Moitra, S. P. Trivedi, and V. Vishal, Extremal and near-extremal black holes and near- CFT_1 , *J. High Energy Phys.* **07** (2019) 055.
- [28] P. Chaturvedi, Y. Gu, W. Song, and B. Yu, A note on the complex SYK model and warped CFTs, *J. High Energy Phys.* **12** (2018) 101.
- [29] T. Faulkner, H. Liu, J. McGreevy, and D. Vegh, Emergent quantum criticality, Fermi surfaces, and AdS_2 , *Phys. Rev. D* **83**, 125002 (2011).
- [30] T. Faulkner, N. Iqbal, H. Liu, J. McGreevy, and D. Vegh, Holographic non-Fermi liquid fixed points, *Phil. Trans. R. Soc. A* **369**, 1640 (2011).
- [31] J. S. Cotler, G. Gur-Ari, M. Hanada, J. Polchinski, P. Saad, S. H. Shenker, D. Stanford, A. Streicher, and M. Tezuka, Black holes and random matrices, *J. High Energy Phys.* **05** (2017) 118.
- [32] A. M. García-García and J. J. M. Verbaarschot, Analytical spectral density of the Sachdev-Ye-Kitaev model at finite N , *Phys. Rev. D* **96**, 066012 (2017).
- [33] D. Bagrets, A. Altland, and A. Kamenev, Power-law out of time order correlation functions in the SYK model, *Nucl. Phys.* **B921**, 727 (2017).
- [34] A. Kitaev and S. J. Suh, Statistical mechanics of a two-dimensional black hole, *J. High Energy Phys.* **05** (2019) 198.
- [35] Y. Gu, A. Kitaev, S. Sachdev, and G. Tarnopolsky, Notes on the complex Sachdev-Ye-Kitaev model, *J. High Energy Phys.* **02** (2020) 157.
- [36] J. Liu and Y. Zhou, Note on global symmetry and SYK model, *J. High Energy Phys.* **05** (2019) 099.
- [37] K. Jensen, S. Kachru, A. Karch, J. Polchinski, and E. Silverstein, Towards a holographic marginal Fermi liquid, *Phys. Rev. D* **84**, 126002 (2011).
- [38] D. Nickel and D. T. Son, Deconstructing holographic liquids, *New J. Phys.* **13**, 075010 (2011).
- [39] S. A. Hartnoll, A. Lucas, and S. Sachdev, *Holographic Quantum Matter* (MIT Press, Cambridge, MA, 2016).
- [40] L. V. Iliesiu, S. Murthy, and G. J. Turiaci, Revisiting the logarithmic corrections to the black hole entropy, [arXiv:2209.13608](https://arxiv.org/abs/2209.13608).
- [41] A. H. Anupam, P. V. Athira, C. Chowdhury, and A. Sen, Logarithmic correction to BPS black hole entropy from supersymmetric index at finite temperature, [arXiv:2306.07322](https://arxiv.org/abs/2306.07322).
- [42] S. Sachdev, Universal low temperature theory of charged black holes with AdS_2 horizons, *J. Math. Phys. (N.Y.)* **60**, 052303 (2019).
- [43] L. V. Iliesiu and G. J. Turiaci, The statistical mechanics of near-extremal black holes, *J. High Energy Phys.* **05** (2021) 145.
- [44] M. Heydeman, L. V. Iliesiu, G. J. Turiaci, and W. Zhao, The statistical mechanics of near-BPS black holes, *J. Phys. A* **55**, 014004 (2022).
- [45] J. Boruch, M. T. Heydeman, L. V. Iliesiu, and G. J. Turiaci, BPS and near-BPS black holes in AdS_5 and their spectrum in $\mathcal{N} = 4$ SYM, [arXiv:2203.01331](https://arxiv.org/abs/2203.01331).
- [46] H. Geng, Aspects of AdS_2 quantum gravity and the Karch-Randall braneworld, *J. High Energy Phys.* **09** (2022) 024.
- [47] G. Ruppeiner, Riemannian geometry in thermodynamic fluctuation theory, *Rev. Mod. Phys.* **67**, 605 (1995); **68**, 313(E) (1996).
- [48] F. Weinhold, Metric geometry of equilibrium thermodynamics, *J. Chem. Phys.* **63**, 2479 (1975); **63**, 2484 (1975).
- [49] H. Janyszek and R. Mrugała, Geometrical structure of the state space in classical statistical and phenomenological thermodynamics, *Rep. Math. Phys.* **27**, 145 (1989).
- [50] J. y. Shen, R. G. Cai, B. Wang, and R. K. Su, Thermodynamic geometry and critical behavior of black holes, *Int. J. Mod. Phys. A* **22**, 11 (2007).

- [51] B. Mirza and M. Zamani-Nasab, Ruppeiner geometry of RN black holes: Flat or curved?, *J. High Energy Phys.* **06** (2007) 059.
- [52] H. Quevedo, Geometrothermodynamics of black holes, *Gen. Relativ. Gravit.* **40**, 971 (2008).
- [53] A. Sahay, T. Sarkar, and G. Sengupta, On the thermodynamic geometry and critical phenomena of AdS black holes, *J. High Energy Phys.* **07** (2010) 082.
- [54] C. Niu, Y. Tian, and X. N. Wu, Critical phenomena and thermodynamic geometry of RN-AdS black holes, *Phys. Rev. D* **85**, 024017 (2012).
- [55] G. Ruppeiner and A. M. Sturzu, Black hole microstructures in the extremal limit, *Phys. Rev. D* **108**, 086004 (2023).
- [56] S. H. Hendi, S. Panahiyan, B. Eslam Panah, and M. Momennia, A new approach toward geometrical concept of black hole thermodynamics, *Eur. Phys. J. C* **75**, 507 (2015).
- [57] S. A. H. Mansoori, B. Mirza, and E. Sharifian, Extrinsic and intrinsic curvatures in thermodynamic geometry, *Phys. Lett. B* **759**, 298 (2016).
- [58] R. Banerjee, S. Ghosh, and D. Roychowdhury, New type of phase transition in Reissner Nordström–AdS black hole and its thermodynamic geometry, *Phys. Lett. B* **696**, 156 (2011).
- [59] G. Ruppeiner, Riemannian geometric approach to critical points: General theory, *Phys. Rev. E* **57**, 5135 (1997).
- [60] J. E. Aman, I. Bengtsson, and N. Pidokrajt, Geometry of black hole thermodynamics, *Gen. Relativ. Gravit.* **35**, 1733 (2003).
- [61] A. Belhaj, M. Chabab, H. El Moumni, K. Masmar, and M. B. Sedra, On thermodynamics of AdS black holes in M-theory, *Eur. Phys. J. C* **76**, 73 (2016).
- [62] K. Bhattacharya and B. R. Majhi, Thermogeometric description of the van der Waals like phase transition in AdS black holes, *Phys. Rev. D* **95**, 104024 (2017).
- [63] S. W. Wei, Y. X. Liu, and R. B. Mann, Repulsive interactions and universal properties of charged anti-de Sitter black hole microstructures, *Phys. Rev. Lett.* **123**, 071103 (2019).
- [64] S. W. Wei, Y. X. Liu, and R. B. Mann, Ruppeiner geometry, phase transitions, and the microstructure of charged AdS black holes, *Phys. Rev. D* **100**, 124033 (2019).
- [65] S. W. Hawking and S. F. Ross, Duality between electric and magnetic black holes, *Phys. Rev. D* **52**, 5865 (1995).
- [66] S. W. Wei, Y. X. Liu, and R. B. Mann, Novel dual relation and constant in Hawking-Page phase transitions, *Phys. Rev. D* **102**, 104011 (2020).
- [67] P. K. Yerra and C. Bhamidipati, Ruppeiner curvature along a renormalization group flow, *Phys. Lett. B* **819**, 136450 (2021).